

Luminescence readout of nanoparticle phase state

A. I. Denisyuk,^{1,a)} F. Jonsson,¹ K. F. MacDonald,¹ N. I. Zheludev,^{1,b)} and F. J. García de Abajo²

¹Optoelectronics Research Centre, University of Southampton, Southampton SO17 1BJ, United Kingdom

²Instituto de Optica, CSIC, Serrano 121, 28006 Madrid, Spain

(Received 23 October 2007; accepted 6 February 2008; published online 5 March 2008)

We report that the phase state of bistable gallium nanoparticles, controlled by optical or electron beam excitations, can be identified via measurements of their cathodoluminescent emission, thus offering an innovative conceptual basis for the development of high density nonvolatile phase-change memories. Changes of up to 20% in visible emission intensity are observed following low-fluence optical or electron beam induced phase switching in a monolayer of 60 nm particles.

© 2008 American Institute of Physics. [DOI: 10.1063/1.2890483]

Phase-change materials, wherein structural forms with differing electronic and/or optical properties are used to encode digital information or control signal propagation, have recently attracted great interest due to their potential to address growing challenges of size and power consumption in data storage and memory applications, and to enable innovative photonic and plasmonic functionalities.^{1–5} Binary and quaternary optical memory functionalities have recently been demonstrated in gallium nanoparticle films and single particles, respectively.^{6,7} In these schemes, single optical pulses induce structural transformations in the particles, thereby “writing” information to the memory element, while “read-out” is achieved through reflective measurements of the particles’ linear or nonlinear optical properties. We report here that the phase (memory) state of gallium nanoparticles can be identified by probing their cathodoluminescent (CL) properties. While this proof-of-principle demonstration addresses a large number of nanoparticles simultaneously, it may ultimately be possible to achieve very high data storage densities if the nanoscale focusing capability of electron beams can be harnessed to address individual particles within an array.

In the experiments reported here, nanoparticle growth, imaging, optical measurements, and CL studies were all performed under high vacuum inside a scanning electron microscope (SEM) equipped with an effusion cell for gallium deposition and a nitrogen-cooled cryostat to control sample temperature in the 100–305 K range [Fig. 1(a)]. Films of gallium nanoparticles were grown on the end faces of cleaved single-mode fibers using the light-assisted self-assembly technique.⁸ With the fiber tip held at a temperature of 100 K, gallium was deposited at 0.3 nm/min for 50 min (giving a mass thickness of 15 nm) while 1 μ s pulses from a 1550 nm diode laser (19 mW, 1 kHz repetition rate) were launched into the fiber from outside the SEM chamber. This process produces a monolayer of particles with a mean diameter of 60 nm on the optical core area of the fiber end face [see Figs. 1(b) and 1(c)]. The integrated experimental system then allows for the particles to be imaged *in situ* by the SEM and for their CL to be probed with the emitted light being directed out of the chamber by a parabolic mirror to a spectrum analyzer (comprising a Horiba Jobin–Yvon CP140

spectrograph and a liquid nitrogen-cooled charged-coupled device array). Furthermore, the nanoparticle films’ reflective optical properties can be studied via the fiber, and phase transitions can be stimulated in the particles by both optical and electron beam excitations.

For the purpose of encoding information in the structural phase of nanoparticles, excitation-induced phase switching is most efficiently performed in the proximity of the phase transition temperature. To identify this temperature for the present case, the reflectivity of the nanoparticle film was recorded as a function of temperature between 100 and 305 K using a continuous-wave 0.5 mW beam from a 1310 nm diode laser [see Fig. 2(a)]. Phase transitions in bulk materials are characterized by a discontinuous change in the state of the body, a sudden (irreversible) rearrangement of the crystalline lattice at a specific temperature. In nanoparticles, however, transitions from lower to higher energy phases proceed through a surface-driven dynamic coexistence of forms across a size-dependent range of temperatures.^{9–11} When the two forms involved have different dielectric coefficients, this gives rise to a continuous change in optical properties, such

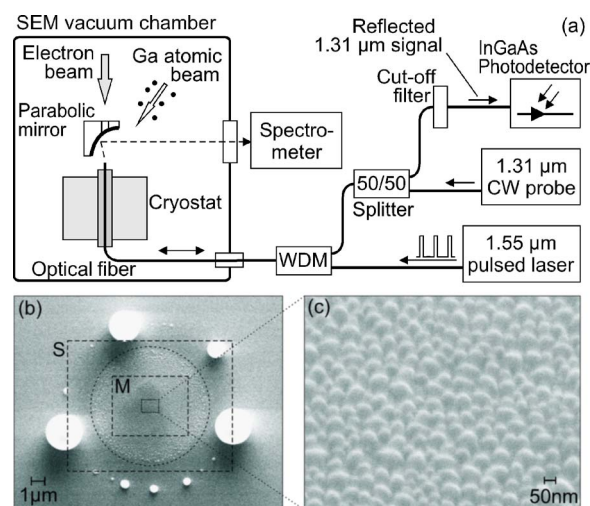


FIG. 1. (Color online) Integrated system for growth, imaging, cathodoluminescence (CL) study, and optical interrogation of gallium nanoparticle films. (b) Secondary electron image of a fiber end face showing the optical core area (dashed circle) where 60 nm particles, shown at higher magnification in (c), are formed during deposition. The dashed squares indicate the areas exposed to electron-beam excitation for CL measurements (M) and to achieve phase switching (S).

^{a)}Electronic mail: aid@soton.ac.uk.

^{b)}Electronic mail: niz@orc.soton.ac.uk. URL: www.nanophotonics.org.uk.

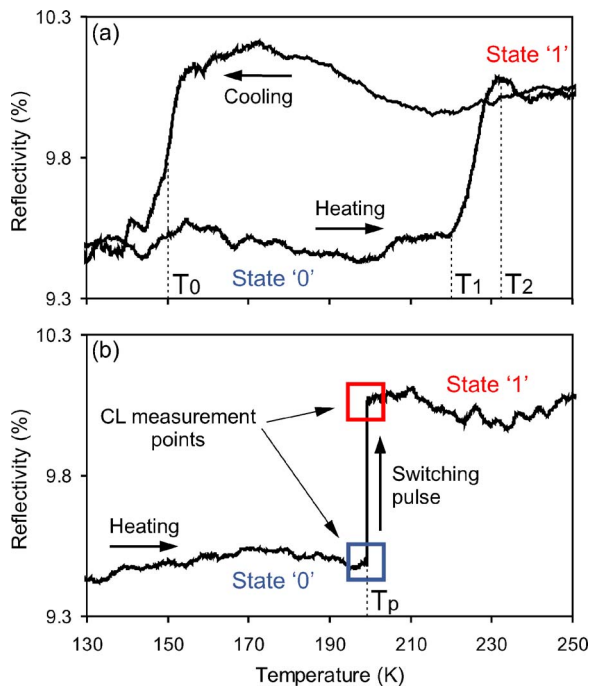


FIG. 2. (Color online) (a) Reflectivity hysteresis of a gallium nanoparticle film on a fiber end face (measured via the fiber) as function of cryostat temperature. (b) Gallium particle film reflectivity as a function of increasing temperature, showing abrupt excitation-induced phase (memory state) switching at $T_p=200$ K ($T_0 < T_p < T_1$). CL measurements are made immediately before and after the induced transition.

as the smooth step change in reflectivity between $T_1 = 220$ K and $T_2 = 233$ K shown in Fig. 2(a), which is associated with the melting of gallium's β crystalline phase^{12,13} (the recorded transition temperature is lower than the listed β -gallium melting point of 257 K due to a combination of size-dependent melting point suppression and a systematic offset linked to the relative positioning of the sensor and fiber tip). With decreasing temperature, the reverse phase transition occurs only after substantial overcooling at $T_0 = 150$ K. This phase bistability underpins the gallium particles' memory functionality.^{6,7}

To demonstrate CL readout of nanoparticle phase (memory) state, a series of experiments was performed. In each case, the nanoparticle film was placed initially in the low reflectivity ("0" logic) solid phase by cooling to the minimum available temperature of about 100 K. Its temperature was then increased and fixed at a point $T_p = 200$ K just below the phase transition point and a CL spectrum was obtained by scanning a $5.5 \times 4.4 \mu\text{m}^2$ region within the core area [square M in Fig. 1(b)] with a low current (< 2.3 nA) electron beam. The nanoparticle film was then switched to the high reflectivity ("1" logic) liquid state by either optical or electron beam excitation. In the former case, a single $1 \mu\text{s}$ pulse from the 1550 nm diode laser with a fluence of ≥ 0.3 fJ/nm² was used to induce a structural phase change. In the latter, switching was initiated by a single 40 ms, 5 keV electron beam scan across a $12 \times 9.6 \mu\text{m}^2$ area encompassing the core [square S in Fig. 1(b)] with a beam current of ≥ 20 nA (a fluence of ≥ 35 fJ/nm²). A second CL measurement was then performed. Throughout this process, and with increasing temperature after the second CL measurement, the reflectivity of the samples was monitored to ensure that the particles' phase state was not switched by the electron

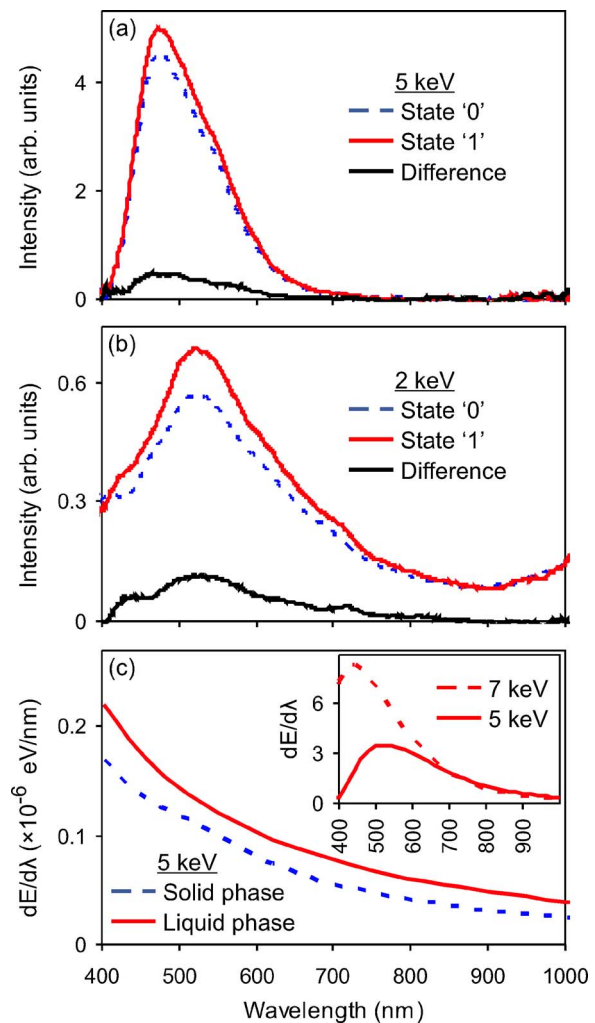


FIG. 3. (Color online) [(a) and (b)] CL spectra of gallium nanoparticle films in solid (0) and liquid (1) states, obtained at a temperature of 200 K before and after excitation-induced switching between the two states, together with the difference spectra. (a) CL spectra obtained with a 5 keV, 2.3 nA electron beam, after subtraction of silica luminescence. (b) CL spectra obtained with a 2 keV, 1 nA beam (silica contribution negligible). (c) Calculated backward transition radiation emission induced by a 5 keV electron beam from 15 nm thick homogeneous solid and liquid gallium films on silica substrates. The inset shows total CL emission (in all directions) from a freestanding, 60 nm diameter spherical particle of liquid gallium in vacuum, performed using the boundary element method, for 5 and 7 keV electron trajectories through the center of the particle.

beam during the first CL measurement and to verify that it was switched abruptly by the excitation pulse prior to the second [see Fig. 2(b)]. The particle film was reset to the solid (0) state by cooling it to below 150 K (recent work has suggested that nanosecond optical pulses could be used to achieve this "memory erase" function at a fixed temperature¹⁴).

CL measurements were performed at 5 and 2 keV electron energies, with beam currents of 2.3 and 1 nA, respectively. Results are shown in Figs. 3(a) and 3(b) with corresponding difference spectra relating to the increase in emission associated with the solid-to-liquid transition in the nanoparticles. The absolute signal intensity is higher at 5 keV because the electrons have a longer penetration depth; however, at this voltage, the recorded spectra contain a significant component relating to the luminescence of the fiber, excited by electrons having passed through the gallium nanoparticle film. This artifact was eliminated via measurements

on a bare fiber tip. At 2 keV, the silica luminescence contribution is negligible and the relative change in signal magnitude on phase switching is larger (20% as compared to 11%). The spectral peaks redshift and broaden with decreasing acceleration voltage, from 475+80/−35 nm at 5 keV to 520+130/−100 nm at 2 keV.

Light emission from metal nanostructures induced by electron bombardment results from a complex combination of several mechanisms, with transition radiation (emitted as electrons cross boundaries between media) and plasmon-mediated emission playing major roles.¹⁵ In the case of gallium, there may also be a contribution from recombination emission because its solid phases show interband transitions [at 520–1000 nm for α -Ga,¹⁶ and 400, 700, and 950 nm for β -Ga (Ref. 17)] via which light can be emitted. Liquid gallium retains some atomic order similar to that of the metastable solid phases¹² and may therefore possess transition bands at similar wavelengths. Numerical models can qualitatively reproduce certain characteristics of the observed emission spectra but no single model can currently account for the full complexity of electron-induced radiation emission from a closely spaced ensemble of truncated spheroidal particles on a substrate (particularly where the exact particle size and geometry are functions of phase state). To a first approximation, a closely packed nanoparticle monolayer may be treated as a homogenous film of equivalent mass thickness (15 nm in the present case). Figure 3(c) shows backward transition radiation emission (integrated over a solid angle of 2π), calculated using formulae from Ref. 18, resulting from 5 keV electron beam excitation of solid and liquid gallium films on silica substrates. (Dielectric constants for β -gallium are not available so values for fractionally disordered α -gallium with optical conductivity similar to β -gallium¹⁹ were used for the solid phase. Dielectric constants for liquid gallium were taken from Ref. 20.) These calculations show higher emission from the liquid phase, as observed experimentally, but do not reproduce the emission peaks shown in Figs. 3(a) and 3(b) because the model does not account for plasmon-mediated emission. Calculations of the total CL emission (in all directions) from a single, free-standing, 60 nm spherical liquid gallium particle in vacuum, performed using the boundary element method,²¹ illustrate the experimentally observed trend for redshifting and broadening of the signal peak with decreasing electron acceleration voltage [see inset to Fig. 3(c)], but such calculations are sensitive to the assumed particle geometry and do not account for interactions between neighboring particles.

The operational energy requirements of nanoparticle-based phase-change memory elements are potentially very low. In a nonvolatile format, they require no holding power and the thermodynamic minimum switching requirement for a β -to-liquid transition in, for example, a 60 nm spherical particle about 30 K below its melting point, is about 35 fJ (based on specific and latent heat values from Ref. 12). While the incident energies per particle used in the present

studies are at least two orders of magnitude higher than this, only a small fraction of the incident energy is actually absorbed by the particle, the rest is reflected or transmitted by the film. Particulate memory elements also offer the possibility of very high data storage densities. For example, if individual binary (two-phase) elements within a close-packed array of 60 nm particles could be addressed, as they might with a steerable tightly focused electron beam, a storage density of ~ 0.2 Tbit/in.² could be achieved (smaller particles and higher-base logical elements⁷ would further increase this value). For comparison, today's "BluRay" disks (based on a chalcogenide phase-change material) offer an optical storage density of just under 0.015 Tbit/in.²

To summarize, it has been shown experimentally that the phase (logic) state of gallium nanoparticle phase-change memory elements can be determined via measurements of their CL emission. Changes of up to 20% in visible emission intensity are observed following low-fluence optical or electron beam induced phase switching of a monolayer of 60 nm particles. This proof of principle investigation demonstrates that electron beam addressed nanoparticles may offer a route toward the development of high density nonvolatile phase-change memories.

The authors would like to acknowledge the support of the Engineering and Physical Sciences Research Council (UK) and EU-FP6 Project No. NMP4-2006-016881 "SPANS."

¹M. Wuttig, *Nat. Mater.* **4**, 265 (2005).

²H. F. Hamann, M. O'Boyle, Y. C. Martin, M. Rooks, and H. K. Wickramasinghe, *Nat. Mater.* **5**, 383 (2006).

³G. A. Gibson, A. Chaiken, K. Nauka, C. C. Yang, R. Davidson, A. Holden, R. Bicknell, B. S. Yeh, J. Chen, H. Liao, S. Subramanian, D. Schut, J. Jasinski, and Z. Liliental-Weber, *Appl. Phys. Lett.* **86**, 051902 (2005).

⁴N. I. Zheludev, *Nat. Photonics* **1**, 551 (2007).

⁵A. V. Krasavin and N. I. Zheludev, *Appl. Phys. Lett.* **84**, 1416 (2004).

⁶B. F. Soares, M. V. Bashevoy, F. Jonsson, K. F. MacDonald, and N. I. Zheludev, *Opt. Express* **14**, 10652 (2006).

⁷B. F. Soares, F. Jonsson, and N. I. Zheludev, *Phys. Rev. Lett.* **98**, 153905 (2007).

⁸K. F. MacDonald, V. A. Fedotov, S. Pochon, K. J. Ross, G. C. Stevens, N. I. Zheludev, W. S. Brocklesby, and V. I. Emel'yanov, *Appl. Phys. Lett.* **80**, 1643 (2002).

⁹R. S. Berry and B. M. Smirnov, *J. Chem. Phys.* **113**, 728 (2000).

¹⁰M. Wautelet, *J. Phys.: Condens. Matter* **16**, L163 (2004).

¹¹P. Buffat and J.-P. Borel, *Phys. Rev. A* **13**, 2287 (1976).

¹²A. Defrain, *J. Chim. Phys. Phys.-Chim. Biol.* **74**, 851 (1977).

¹³A. Di Cicco, *Phys. Rev. Lett.* **81**, 2942 (1998).

¹⁴B. F. Soares, K. F. MacDonald, and N. I. Zheludev, *Appl. Phys. Lett.* **91**, 043115 (2007).

¹⁵N. Yamamoto, K. Araya, A. Toda, and H. Sugiyama, *Surf. Interface Anal.* **31**, 79 (2001).

¹⁶O. Hunderi and R. Ryberg, *J. Phys. F: Met. Phys.* **4**, 2084 (1974).

¹⁷O. Hunderi, *J. Phys. F: Met. Phys.* **5**, 883 (1975).

¹⁸V. E. Pafomov and I. M. Frank, *Sov. J. Nucl. Phys.* **5**, 448 (1967).

¹⁹O. Hunderi and R. Ryberg, *J. Phys. F: Met. Phys.* **4**, 2096 (1974).

²⁰R. S. Teshev and A. A. Shebzukhov, *Opt. Spectrosc.* **65**, 693 (1988).

²¹F. J. Garca de Abajo and A. Howie, *Phys. Rev. B* **65**, 115418 (2002).